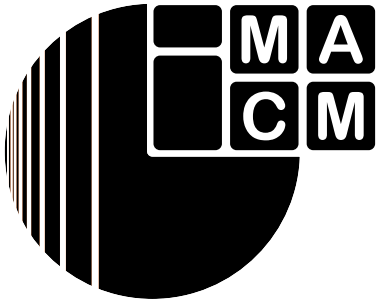

Bergische Universität Wuppertal

Fachbereich Mathematik und Naturwissenschaften

Institute of Mathematical Modelling, Analysis and Computational Mathematics (IMACM)

Preprint BUW-IMACM 16/19

Dmitry Shcherbakov, Matthias Ehrhardt,Jacob Finkenrath, Michael Günther, Francesco Knechtli, Michael Peardon

Adapted nested force-gradient integrators: the Schwinger model case

October 18, 2016

http://www.math.uni-wuppertal.de

Adapted nested force-gradient integrators: the Schwinger model case

Dmitry Shcherbakov[1,*], Matthias Ehrhardt[1], Jacob Finkenrath[2], Michael Günther[1], Francesco Knechtli[3] and Michael Peardon[4]

[1] *Lehrstuhl für Angewandte Mathematik und Numerische Analysis, Bergische Universität Wuppertal, Gaußstrasse 20, 42119 Wuppertal, Germany*
[2] *CaSToRC, CyI, 20 Constantinou Kavafi Street, 2121 Nicosia, Cyprus*
[3] *Theoretische Physik, Bergische Universität Wuppertal, Gaußstrasse 20, 42119 Wuppertal, Germany*
[4] *School of Mathematics, Trinity College, Dublin 2, Ireland*

Abstract. We study a novel class of numerical integrators, the adapted nested force-gradient schemes, used within the molecular dynamics step of the Hybrid Monte Carlo (HMC) algorithm. We test these methods in the Schwinger model on the lattice, a well known benchmark problem. We derive the analytical basis of nested force-gradient type methods and demonstrate the advantage of the proposed approach, namely reduced computational costs compared with other numerical integration schemes in HMC.

AMS subject classifications: 65P10 65L06 34C40

Key words: numerical geometric integration, decomposition methods, energy conservation, force-gradient, nested algorithms, multi-rate schemes, operator splitting, Schwinger model

1 Introduction

For the Hybrid Monte Carlo algorithm (HMC) [5], often used to study quantum chromodynamics (QCD) on the lattice, one is interested in efficient numerical time integration schemes which are optimal in terms of computational costs per trajectory for a given acceptance rate. High order numerical methods allow the use of larger step sizes, but demand a larger computational effort per step; low order schemes do not require such large computational costs per step, but need more steps per trajectory. So there is a need to balance these opposing effects.

*Corresponding author. *Email addresses:* shcherbakov@math.uni-wuppertal.de (D. Shcherbakov), ehrhardt@math.uni-wuppertal.de (M. Ehrhardt),j.finkenrath@cyi.ac.cy (J. Finkenrath), guenther@math.uni-wuppertal.de (M. Günther), knechtli@physik.uni-wuppertal.de (F. Knechtli), mjp@maths.tcd.ie (M. Peardon)

Omelyan integration schemes [11] of a force-gradient type have proved to be an efficient choice, since it is easy to obtain higher order schemes that demand a small additional computational effort. These schemes use higher-order information from force-gradient terms to both increase the convergence of the method and decrease the size of the leading error coefficient. Other ideas to achieve better efficiency for numerical time integrators are given by multirate or nested approaches. These schemes do not increase the order but reduce the computational costs per path by recognizing the different dynamical time-scales generated by different parts of the action. Slow forces, which are usually expensive to evaluate, need only to be sampled at low frequency while fast forces which are usually cheap to evaluate need to be sampled at a high frequency. A natural way to inherit the advantages from both force-gradient type schemes and multirate approaches would be to combine these two ideas.

Previously, we studied the behavior of the adapted nested force-gradient scheme for the example of the n-body problem [15] and would like to learn more about their usefulness for lattice field theory calculations. Due to the huge computational effort required for QCD simulations, it is natural to attempt an intermediate step first. We chose the model problem of quantum electrodynamics (QED) in two dimensions, the Schwinger model [12], since it is well-suited as a test case for new concepts and ideas which can be subsequently applied to more computationally demanding problems [4]. As a lattice quantum field theory, it has many of the properties of more sophisticated models such as QCD, for example the numerical cost is still dominated by the fermion part of the action. The fact that this model, with far fewer degrees of freedom, does not require such large computational effort makes it the perfect choice for testing purposes.

We compare the behavior of numerical time integration schemes currently used for HMC [11] with the nested force-gradient integrator [3] and the adapted version introduced in [15]. We investigate the computational costs needed to perform numerical calculations, as well as the effort required to achieve a satisfactory acceptance rate during the HMC evolution. Our goal is to find a numerical scheme for the HMC algorithm which would provide a sufficiently high acceptance rate while not drastically increasing the simulation time.

The paper is organized as follows. In Section 2 we give a short overview of the HMC algorithm and numerical schemes for time integration, which are used in HMC. In Section 3 we present the 2-dimensional Schwinger model and introduce the idea of the force-gradient approach and the resulting novel class of numerical schemes. Section 4 is devoted to the results of a comparison between widely used algorithms and the new approach and Section 5 draws our conclusion.

2 Geometric integrators for HMC

In this section we provide a general overview of the HMC algorithm [5] to introduce our novel integrator. We also present some standard numerical time integrating methods used in HMC, as well state-of-the-art numerical schemes, which we later compare by applying them to the two-dimensional Schwinger model.

2.1 Overview of HMC

In the Hybrid Monte Carlo algorithm, the quantum lattice field theory is embedded in a higher-dimensional classical system through the introduction of a fictitious (simulation) time [5]. The gauge field U is associated with its (fictitious) conjugate momenta P, and the classical system is described by the Hamiltonian,

$$H = \mathcal{A}[P] + \mathcal{B}[U], \tag{2.1}$$

where $\mathcal{A}[P]$ and $\mathcal{B}[U]$ represent the kinetic and potential energy respectively.

For a given configuration U, a new configuration U' is generated by performing an HMC update $U \to U'$, which consists of two steps:

- **Molecular Dynamics trajectory:** Evolve the gauge fields U, elements of a Lie group, and the momenta P, elements of the corresponding Lie algebra, in a fictitious computer time t according to Hamilton's equations of motions

$$\dot{P} = -\frac{\partial H}{\partial U} = -F_V(U), \qquad\qquad \dot{U} = PU. \tag{2.2}$$

  Since analytical solutions are not available in general, numerical methods must be used to solve the system of Eqn. (2.2). The discrete updates of U and P with an integration step h are

$$\begin{aligned} e^{\mathcal{A}h}&: \; U \;\to\; U' = \exp(iPh)U \\ e^{\mathcal{B}h}&: \; P \;\to\; P' = P - ihF_V(U), \end{aligned}$$

  leading to a first-order approximation at time $t+h$. Since the momenta P are elements of Lie algebra, we have an additive update of P. On the other hand, the links U must be elements of the Lie group, therefore an exponential update is used for U to preserve the underlying group structure.

- **Metropolis step:** Accept or reject the new configuration (U', P') with probability

$$\mathcal{P}(U \to U') = \min\left(1, e^{-\Delta H}\right),$$

  where $\Delta H = H(U', P') - H(U, P)$.

2.2 Integrators used for Molecular Dynamics

In this paper we are concerned with numerical time integration schemes, which preserve the fundamental properties of geometric integration, time-reversibility and volume-preservation. All numerical schemes presented below possess these necessary properties.

Basic schemes: Well-known, commonly used integration schemes in molecular dynamics are given by

- the leap-frog method, a 3-stage composition scheme of the discrete updates defined above:

$$\Delta(h) = \mathrm{e}^{h\frac{\hat{\mathcal{B}}}{2}}\mathrm{e}^{h\hat{\mathcal{A}}}\mathrm{e}^{h\frac{\hat{\mathcal{B}}}{2}}, \tag{2.3}$$

- and a 5-stage extension widely used in QCD computations:

$$\Delta_5(h) = \mathrm{e}^{\frac{1}{6}h\hat{\mathcal{B}}}\mathrm{e}^{\frac{1}{2}h\hat{\mathcal{A}}}\mathrm{e}^{\frac{2}{3}h\hat{\mathcal{B}}}\mathrm{e}^{\frac{1}{2}h\hat{\mathcal{A}}}\mathrm{e}^{\frac{1}{6}h\hat{\mathcal{B}}}. \tag{2.4}$$

Force gradient schemes: Force-gradient schemes increase accuracy by using additional information from the force gradient term $\mathcal{C} = \{\mathcal{B},\{\mathcal{A},\mathcal{B}\}\}$, with $\{\ ,\ \}$ defining Lie brackets. The 5-stage force-gradient scheme proposed by Omelyan et al [11] is the simplest;

$$\Delta_{5C}(h) = \mathrm{e}^{\frac{1}{6}h\hat{\mathcal{B}}}\mathrm{e}^{\frac{1}{2}h\hat{\mathcal{A}}}\mathrm{e}^{\frac{2}{3}h\hat{\mathcal{B}}-\frac{1}{72}h^3\mathcal{C}}\mathrm{e}^{\frac{1}{2}h\hat{\mathcal{A}}}\mathrm{e}^{\frac{1}{6}h\hat{\mathcal{B}}}. \tag{2.5}$$

Here we also test the modification of the force-gradient method (2.5) proposed in [17], where the force-gradient term $\mathcal{C}$ is approximated via a Taylor expansion. An extension is given by the 11-stage decomposition [11], recently implemented as the integrator in the open source code openQCD as one of the standard options [10]

$$\Delta_{11}(h) = \mathrm{e}^{\sigma h\hat{\mathcal{B}}}\mathrm{e}^{\eta h\hat{\mathcal{A}}}\mathrm{e}^{\lambda h\hat{\mathcal{B}}}\mathrm{e}^{\theta h\hat{\mathcal{A}}}\mathrm{e}^{(1-2(\lambda+\sigma))\frac{h}{2}\hat{\mathcal{B}}}\mathrm{e}^{(1-2(\theta+\eta))h\hat{\mathcal{A}}}\mathrm{e}^{(1-2(\lambda+\sigma))\frac{h}{2}\hat{\mathcal{B}}}\mathrm{e}^{\theta h\hat{\mathcal{A}}}\mathrm{e}^{\lambda h\hat{\mathcal{B}}}\mathrm{e}^{\eta h\hat{\mathcal{A}}}\mathrm{e}^{\sigma h\hat{\mathcal{B}}}, \tag{2.6}$$

where σ, θ, λ and η are parameters from equation (71) in Ref. [11].

Nested Schemes: QED and QCD problems usually lead to Hamiltonians with the following fine structure

$$H = \mathcal{A}[P] + \mathcal{B}_1[U] + \mathcal{B}_2[U], \tag{2.7}$$

where the action of the system can be split into two parts: a fast action $\mathcal{B}_1$ such as the gauge action, and a slow part $\mathcal{B}_2$, for example, the fermion action. This allows us to apply the idea of multirate schemes (an idea known as nested integration in physics literature) [13] in order to reduce the computational effort. At first we consider the nested version of the leap-frog method (2.3)

$$\hat{\Delta}(h) = \mathrm{e}^{\frac{h}{2}\hat{\mathcal{B}}_2}\Delta_1(h)_M\mathrm{e}^{\frac{h}{2}\hat{\mathcal{B}}_2}, \tag{2.8}$$

where the inner cheaper system $H = \mathcal{A}[P] + \mathcal{B}_1[U]$ is solved by

$$\Delta_1(h)_M = \left(\mathrm{e}^{\frac{h}{2M}\hat{\mathcal{B}}_1}\mathrm{e}^{\frac{h}{M}\hat{\mathcal{A}}}\mathrm{e}^{\frac{h}{2M}\hat{\mathcal{B}}_1}\right)^M,$$

with M being a number of iterations for the fast part of the action. Our main goal is to compare the above-mentioned methods with more elaborated nested schemes: in [15], a similar 5-stage decomposition scheme has been recently introduced:

$$\hat{\Delta}_5(h) = \mathrm{e}^{\frac{1}{6}h\hat{\mathcal{B}}_2}\Delta_1\left(\frac{h}{2}\right)_M\mathrm{e}^{\frac{2}{3}h\hat{\mathcal{B}}_2}\Delta_1\left(\frac{h}{2}\right)_M\mathrm{e}^{\frac{1}{6}h\hat{\mathcal{B}}_2}. \tag{2.9}$$

A nested version of (2.5), which has been used in [1] reads

$$\hat{\Delta}_{5C}(h) = \mathrm{e}^{\frac{1}{6}h\hat{\mathcal{B}}_2}\Delta_2\left(\frac{h}{2}\right)_M\mathrm{e}^{\frac{2}{3}h\hat{\mathcal{B}}_2+\frac{1}{72}h^3\mathcal{C}_f}\Delta_2\left(\frac{h}{2}\right)_M\mathrm{e}^{\frac{1}{6}h\hat{\mathcal{B}}_2}, \tag{2.10}$$

where

$$\Delta_2(h)_M = \left(\mathrm{e}^{\frac{1}{6M}h\hat{\mathcal{B}}_1} \mathrm{e}^{\frac{1}{2M}h\hat{\mathcal{A}}} \mathrm{e}^{\frac{2}{3M}h\hat{\mathcal{B}}_1 + \frac{1}{72}\left(\frac{h}{M}\right)^3 \mathcal{C}_g} \mathrm{e}^{\frac{1}{2M}h\hat{\mathcal{A}}} \mathrm{e}^{\frac{1}{6M}h\hat{\mathcal{B}}_1} \right)^M,$$

with $\mathcal{C}_g = \{\mathcal{B}_1, \{\mathcal{A}, \mathcal{B}_1\}\}$ and $\mathcal{C}_f = \{\mathcal{B}_2, \{\mathcal{A}, \mathcal{B}_2\}\}$. In the limit $M \to \infty$ we have $\Delta_1 = \Delta_2$. Note that this approach uses force-gradient information at all levels, i.e., the high computational cost of high order schemes appears at all levels.

One may overcome this problem by using schemes of different order at the different levels without losing the effective high order of the overall multirate scheme. For the latter, we include appropriate force gradient information as we explain in the following for the case of two time levels, where the gauge action plays the role of the fast and cheap part, and the fermionic action plays the role of the slow and expensive part. The reasoning is as follows: if one uses the 5-stage Sexton-Weingarten integrator of second order for the slow action, and approximates the fast action by m Leap-frog steps of step size $h/(2m)$, the error of the overall multirate scheme will be of order $\mathcal{O}(h^2) + \mathcal{O}((\frac{h}{m})^2) + \mathcal{O}(h^4)$. With the use of force gradient information only at the slowest level it is possible to cancel the leading error term of order $\mathcal{O}(h^2)$. As $m \geq \frac{1}{h}$ usually holds in the multirate setting, the overall order is then given by the leading error term of order $\mathcal{O}(h^4)$, i.e., the scheme has an effective order of four. One example for such a scheme for problems of type (2.7) is given by the 5-stage nested force-gradient scheme introduced in [15]

$$\tilde{\Delta}_{5C}(h) = \mathrm{e}^{\frac{1}{6}h\hat{\mathcal{B}}_2} \Delta_1\left(\frac{h}{2}\right)_M \mathrm{e}^{\frac{2}{3}h\hat{\mathcal{B}}_2 + \frac{1}{72}h^3\mathcal{C}_f} \Delta_1\left(\frac{h}{2}\right)_M \mathrm{e}^{\frac{1}{6}h\hat{\mathcal{B}}_2}. \tag{2.11}$$

To summarize, the adapted scheme (2.11) differs from the original one (2.10) in two perspectives:

- The force gradient scheme for the fast action is replaced by a leap-frog scheme.
- Only the part $\{\mathcal{B}_2, \{\mathcal{A}, \mathcal{B}_2\}\}$ of the full force gradient $\{\mathcal{B}_1 + \mathcal{B}_2, \{\mathcal{A}, \mathcal{B}_1 + \mathcal{B}_2\}\}$ is needed to gain the effective order of four.

The numerical schemes (2.3)-(2.4) and (2.8)-(2.9) are second order convergent schemes. Methods (2.5)-(2.6) and (2.10) - (2.11) have the fourth order of convergence. We do not consider integrators of higher order than four since the computational costs are too high. The schemes of the same convergence order differ from each other by the number of stages (updates of momenta and links per time step). Usually methods with more stages have smaller leading error coefficients and therefore have better accuracy, but higher computational costs. We would like to determine which integrator would represent the best compromise between high accuracy and computational efficiency.

We will apply all these numerical integration schemes (2.3)–(2.11) to the two-dimensional Schwinger model. The most challenging task from the theoretical point of view is to derive the force-gradient term $\mathcal{C}$. In the next section we introduce the Schwinger model and explain how to obtain the force-gradient term.

3 The Schwinger model and its force gradient terms

The 2 dimensional Schwinger model is defined by the following Hamiltonian function

$$H=\frac{1}{2}\sum_{n=1,\mu=1}^{V,2}p_{n,\mu}^2+S_{full}[U]=\frac{1}{2}\sum_{n=1,\mu=1}^{V,2}p_{n,\mu}^2+S_G[U]+S_F[U]. \tag{3.1}$$

with $V=L\times T$ the volume of the lattice. Unlike QCD, where $U\in SU(3)$ and $p_{n,\mu}\in su(3)$, for this QED problem (3.1), the links U are the elements of the Lie group $U(1)$ and the momenta $p_{n,\mu}$ belong to $\mathbb{R}$, which represents the Lie algebra of the group $U(1)$. This makes this test example (3.1) very cheap in terms of the computational time. This together with the fact that the Schwinger model also shares many of the features of QCD simulations, makes the Schwinger model an excellent test example when considering numerical integrators: a fast dynamics given by the computationally cheap gauge part $S_G[U]$ of the action demanding small step sizes, and a slow dynamics given by the computationally expensive fermion part $S_F[U]$ allowing large step sizes.

The pure gauge part of the action S_G sums up over all plaquettes $\mathbb{P}(n)$ in the two-dimensional lattice with

$$\mathbb{P}(n)=U_1(n)U_2(n+\hat{1})U_1^\dagger(n+\hat{2})U_2^\dagger(n),$$

and is given by

$$S_G=\beta\sum_{n=1}^{V}(1-\mathrm{Re}\mathbb{P}(n)). \tag{3.2}$$

The links U can be written in the form $U_\mu(n)=e^{iq_\mu(n)}\in \mathrm{U}(1)$ and connect the sites n and $n+\hat{\mu}$ on the lattice; $q_\mu(n)\in[-\pi,\pi]$, μ, $\nu\in\{x,t\}$ are respectively space and time directions and β is a coupling constant. Note that from now on we will set the lattice spacing $a=1$.

The fermion part of the action S_F is given by

$$S_F=\eta^\dagger\left(D^\dagger D\right)^{-1}\eta, \tag{3.3}$$

where η is a complex pseudofermion field. Here, D denotes the Wilson–Dirac operator given by

$$D_{n,m}=(2+m_0)\delta_{n,m}-\frac{1}{2}\sum_{\mu=1}^{2}\left((1-\sigma_\mu)U_\mu(n)\delta_{n,m-\hat{\mu}}+(1+\sigma_\mu)U_\mu^\dagger(n-\hat{\mu})\delta_{n,m+\hat{\mu}}\right),$$

where σ_μ are the Pauli matrices

$$\sigma_1=\begin{pmatrix}0&1\\1&0\end{pmatrix}\ \text{and}\ \sigma_2=\begin{pmatrix}0&-i\\i&0\end{pmatrix}.$$

m_0 is the mass parameter and the Kronecker delta $\delta_{n,m}$ acts on the pseudofermion field by $\sum_{m=1}^{V}\delta_{n,m}\eta(m)=\eta(n)$ with $\eta(n)$ the pseudofermion field, a vector in the two-dimensional spinor space taking values at each lattice point n. In order to proceed with the numerical integration we need to obtain the force F and the force gradient term $\mathcal{C}$. The force term $F(n,\mu)$ with respect to the link $U_\mu(n)$ is given by the first derivative of the action S_{full} and can be written as

$$F(n,\mu)=F_{S_G}(n,\mu)+F_{S_F}(n,\mu)=\frac{\partial S_G}{\partial q_\mu(n)}+\frac{\partial S_F}{\partial q_\mu(n)}. \tag{3.4}$$

Since the numerical schemes (2.9)–(2.11) use the multi-rate approach, the shifts in the momenta updates are split on F_{S_G} and F_{S_F} and we can consider them separately. The force terms F_{S_G} and F_{S_F} are obtained by differentiation over $U(1)$ group elements, which for the Schwinger model is the standard differentiation.

The force associated with link $U_\mu(n)$ from the gauge action is given by

$$\beta g(n,\mu):=F_{S_G}(n,\mu)=\beta\,\mathrm{Im}\left(\mathbb{P}(n)-\mathbb{P}(n-\hat{\nu})\right)\big|_{\mu\neq\nu}. \tag{3.5}$$

The force term of the fermion part is given by

$$f(n,\mu):=F_{S_F}=-\mathrm{Im}\left[\chi^\dagger(n)(1-\sigma_\mu)U_\mu(n)\xi(n+\hat{\mu})-\chi^\dagger(n+\hat{\mu})(1+\sigma_\mu)U_\mu^\dagger(n)\xi(n)\right] \tag{3.6}$$

where vectors χ and ξ are given

$$\chi=D^{\dagger^{-1}}\eta, \qquad\qquad \xi=D^{-1}D^{\dagger^{-1}}\eta. \tag{3.7}$$

For the numerical methods (2.5) and (2.10) we need to find the force gradient term $\mathcal{C}(n,\mu)$ with respect to the link $U_\mu(n)$. In case of the Schwinger model (2.1) this term reads

$$\mathcal{C}(n,\mu)=2\sum_{m=1,\nu=1}^{V,2}\frac{\partial S_{full}}{\partial q_\nu(m)}\frac{\partial^2 S_{full}}{\partial q_\nu(m)\partial q_\mu(n)}. \tag{3.8}$$

For simplicity we decompose the force gradient term (3.8) in four parts

$$\begin{aligned}
\mathcal{C}_{GG}&=2\sum_{m=1,\nu=1}^{V,2}\frac{\partial S_G}{\partial q_\nu(m)}\frac{\partial^2 S_G}{\partial q_\nu(m)\partial q_\mu(n)}, \quad \mathcal{C}_{FG}=2\sum_{m=1,\nu=1}^{V,2}\frac{\partial S_F}{\partial q_\nu(m)}\frac{\partial^2 S_G}{\partial q_\nu(m)\partial q_\mu(n)},\\
\mathcal{C}_{GF}&=2\sum_{m=1,\nu=1}^{V,2}\frac{\partial S_G}{\partial q_\nu(m)}\frac{\partial^2 S_F}{\partial q_\nu(m)\partial q_\mu(n)}, \quad \mathcal{C}_{FF}=2\sum_{m=1,\nu=1}^{V,2}\frac{\partial S_F}{\partial q_\nu(m)}\frac{\partial^2 S_F}{\partial q_\nu(m)\partial q_\mu(n)}.
\end{aligned} \tag{3.9}$$

This decomposition is also useful since the numerical integrator (2.10) only uses the term $\mathcal{C}_{FF}$ by construction. As shown in [15], to obtain the fourth order convergent scheme (2.10) from the second order convergent method (2.9) we must eliminate the leading error term, which is exactly represented by $\mathcal{C}_{FF}$. For completeness we discuss all 4 parts below.

The $\mathcal{C}_{GG}$ part of the force-gradient term is

$$\begin{aligned}\mathcal{C}_{GG} = 2\beta^2 [&\mathrm{Im}(4\mathbb{P}_1(n,\mu) - \mathbb{P}_2(n,\mu) - \mathbb{P}_3(n,\mu) - \mathbb{P}_4(n,\mu) - \mathbb{P}_5(n,\mu))\mathrm{Re}(\mathbb{P}_1(n,\mu)) \\ &- \mathrm{Im}(4\mathbb{P}_2(n,\mu) - \mathbb{P}_1(n,\mu) - \mathbb{P}_6(n,\mu) - \mathbb{P}_7(n,\mu) - \mathbb{P}_8(n,\mu))\mathrm{Re}(\mathbb{P}_2(n,\mu))]\end{aligned}$$

with the set of plaquettes

$$\begin{aligned}\mathbb{P}_1(n,\mu) &= U_\mu(n)U_\nu(n+\hat{\mu})U_\mu^\dagger(n+\hat{\nu})U_\nu^\dagger(n), \\ \mathbb{P}_2(n,\mu) &= U_\mu(n-\hat{\nu})U_\nu(n-\hat{\nu}+\hat{\mu})U_\mu^\dagger(n)U_\nu^\dagger(n-\hat{\nu}), \\ \mathbb{P}_3(n,\mu) &= U_\mu(n+\hat{\mu})U_\nu(n+2\hat{\mu})U_\mu^\dagger(n+\hat{\nu}+\hat{\mu})U_\nu^\dagger(n+\hat{\mu}), \\ \mathbb{P}_4(n,\mu) &= U_\mu(n+\hat{\nu})U_\nu(n+\hat{\mu}+\hat{\nu})U_\mu^\dagger(n+2\hat{\nu})U_\nu^\dagger(n+\hat{\nu}), \\ \mathbb{P}_5(n,\mu) &= U_\mu(n-\hat{\mu})U_\nu(n)U_\mu^\dagger(n+\hat{\nu}-\hat{\mu})U_\nu^\dagger(n-\hat{\mu}), \\ \mathbb{P}_6(n,\mu) &= U_\mu(n-\hat{\mu}-\hat{\nu})U_\nu(n-\hat{\nu})U_\mu^\dagger(n-\hat{\mu})U_\nu^\dagger(n-\hat{\mu}-\hat{\nu}), \\ \mathbb{P}_7(n,\mu) &= U_\mu(n-2\hat{\nu})U_\nu(n-2\hat{\nu}+\hat{\mu})U_\mu^\dagger(n-\hat{\nu})U_\nu^\dagger(n-2\hat{\nu}), \\ \mathbb{P}_8(n,\mu) &= U_\mu(n-\hat{\nu}+\hat{\mu})U_\nu(n-\hat{\nu}+2\hat{\mu})U_\mu^\dagger(n+\hat{\mu})U_\nu^\dagger(n-\hat{\nu}+\hat{\mu}).\end{aligned}$$

Then by using the vectors $f(n,\mu)$ defined in (3.6) we obtain the $\mathcal{C}_{FG}$ piece of the force-gradient term given by

$$\begin{aligned}\mathcal{C}_{FG}(n,\mu) = 2\beta [&(f(n,\mu) + f(n+\hat{\mu},\nu) - f(n+\hat{\nu},\mu) - f(n,\nu))\mathrm{Re}(\mathbb{P}_1) \\ &+ (f(n,\mu) - f(n+\hat{\mu}-\hat{\nu},\nu) - f(n-\hat{\nu},\mu) + f(n-\hat{\nu},\nu))\mathrm{Re}(\mathbb{P}_2)].\end{aligned}$$

The second derivative of the fermion action is

$$\begin{aligned}&\frac{\partial^2 S_F}{\partial q_\nu(m)\partial q_\mu(n)} = \\ &2\mathrm{Re}\chi^\dagger \left[\frac{\partial D}{\partial q_\nu(m)} D^{-1} \frac{\partial D}{\partial q_\mu(n)} + \frac{\partial D}{\partial q_\mu(n)} D^{-1} \frac{\partial D}{\partial q_\nu(m)} - \frac{\partial^2 D}{\partial q_\nu(m)\partial q_\mu(n)}\right]\xi + \\ &2\mathrm{Re}\chi^\dagger \frac{\partial D}{\partial q_\mu(n)} (D^\dagger D)^{-1} \frac{\partial D^\dagger}{\partial q_\nu(m)}\chi, \\ &= 2\mathrm{Re}\left[z_{1,m,\nu}^\dagger \frac{\partial D}{\partial q_\mu(n)}\xi + \chi^\dagger \frac{\partial D}{\partial q_\mu(n)} D^{-1} w_{2,m,\nu} - \chi^\dagger \frac{\partial^2 D}{\partial q_\nu(m)\partial q_\mu(n)}\xi + \chi^\dagger \frac{\partial D}{\partial q_\mu(n)} D^{-1} z_{1,m,\nu}\right] \\ &= 2\mathrm{Re}\left[z_{1,m,\nu}^\dagger w_{2,n,\mu} + w_{1,n,\mu}^\dagger z_{2,m,\nu} - \chi^\dagger \frac{\partial^2 D}{\partial q_\nu(m)\partial q_\mu(n)}\xi\right] \qquad (3.10)\end{aligned}$$

in terms of the vectors χ and ξ defined in (3.7). Now the fields $z_{1,m,\nu}$ and $z_{2,m,\nu}$ are given by

$$\begin{aligned}z_{1,m,\nu} &:= D^{\dagger^{-1}} \frac{\partial D^\dagger}{\partial q_\nu(m)}\chi = D^{\dagger^{-1}} w_{1,m,\nu} \\ z_{2,m,\nu} &:= D^{-1}\left(\frac{\partial D}{\partial q_\nu(m)}\xi + z_{1,m,\nu}\right) = D^{-1}(w_{2,m,\nu} + z_{1,m,\nu})\end{aligned}$$

with

$$w_{1,m,\nu}(n) := \sum_{n'} \frac{\partial D^{\dagger}_{n,n'}}{\partial q_\nu(m)} \chi(n') = \delta_{n,m+\hat{\nu}} \frac{i}{2}(1-\sigma_\nu) U^{\dagger}_\nu(m)\chi(m) - \delta_{n,m} \frac{i}{2}(1+\sigma_\nu) U_\nu(m)\chi(m+\hat{\nu}),$$
$$w_{2,m,\nu}(n) := \sum_{n'} \frac{\partial D_{n,n'}}{\partial q_\nu(m)} \xi(n') = -\delta_{n,m} \frac{i}{2}(1-\sigma_\nu) U_\nu(m)\xi(m+\hat{\nu}) + \delta_{n,m+\hat{\nu}} \frac{i}{2}(1+\sigma_\nu) U^{\dagger}_\nu(m)\xi(m).$$

In order to calculate C_{GF} and C_{FF} it is possible to perform the summation of $\sum_{m,\nu}$ before the inversions of D and $D^{\dagger}$ to get z_1 and z_2 which save $\mathcal{O}(V)$ additional inversions for the force gradient terms. It follows for the force gradient term C_{FF}

$$\mathcal{C}_{FF}(n,\mu) = 4\mathrm{Re}\left[Z_1^{\dagger} w_{2,n,\mu} + w^{\dagger}_{1,n,\mu} Z_2 - \chi^{\dagger} \frac{\partial^2 D}{\partial q_\mu(n) \partial q_\mu(n)} \xi \cdot f(n,\mu) \right] \tag{3.11}$$

with

$$\begin{aligned} Z_1 &:= D^{\dagger^{-1}} \sum_{m=1,\nu=1}^{V,2} \left(w_{1,m,\nu} \cdot f(m,\nu) \right), \\ Z_2 &:= D^{-1} \left(\sum_{m=1,\nu=1}^{V,2} [w_{2,m,\nu} \cdot f(m,\nu)] + Z_1 \right). \end{aligned} \tag{3.12}$$

The expression for C_{GF} can be obtained from the one for C_{FF} by replacing in (3.11) and (3.12) the vector f with βg defined in (3.5).

It is important to mention that the computationally most demanding part of the numerical integration of the Schwinger model and quantum field theory in general is the inverse of the Dirac operator D^{-1}. Every momenta update, which includes fermion action (3.6) requires 2 inversions of the Dirac operator, the addition of the force-gradient term $\mathcal{C}$ requires 4 more inversions. Therefore leap-frog based methods (2.3) and (2.8) need 4 computations of D^{-1} per time step; schemes (2.4) and (2.9) 6 times; force-gradient based methods 8 for (2.10) and (2.11), 10 for (2.5) and the 11 stage method (2.6) has 12 inversions of the Dirac operator. Since we use the multi-rate approach for schemes (2.9), (2.10) and (2.11), which leads generally to fewer macro time steps needed than for the standard schemes we expect the integrator (2.11) will be the most efficient choice among the methods considered. In the next section we present numerical tests of this prediction.

4 Numerical results

In this section we apply the numerical integrators (2.3) – (2.11) to compute the molecular dynamics step for the Schwinger model (3.1) when studied with the HMC algorithm. We consider a 32 by 32 lattice with a coupling constant $\beta = 1.0$ and mass $m_0 = -0.231367$. The parameters were taken from [4] and correspond to the scaling variable $z = 0.2$ defined in [4].We have chosen them to simulate close to the scaling limit with light fermions and also to increase the impact of the fermion part of the action. We

use one thermalised gauge configuration. For each integrator and value of the step-size we generate 200 independent sets of momenta and integrate the equations of motion on a trajectory of length $\tau = 2.0$. We compute the absolute error $|\Delta H|$ and estimate its statistical error from the standard deviation. Also the parameter M is chosen in such a way to make micro step size to be 10 times smaller than the macro step size h.

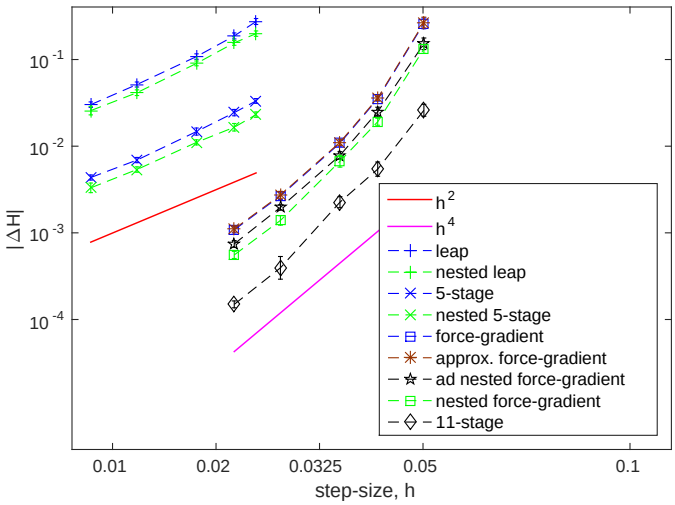

Figure 1: Absolute error for different numerical integrators.

Figure 1 presents the comparison between the numerical integrators (2.3) – (2.11). It shows the absolute error $|\Delta H|$ versus the step-size of the numerical scheme. Here the multi-rate schemes (2.8), (2.9), (2.10) and (2.11) outperform their standard versions as expected. Also it is easy to see that the scheme (2.6) has the best accuracy and the nested force-gradient method (2.10) just slightly edges the adapted nested force-gradient scheme (2.11).

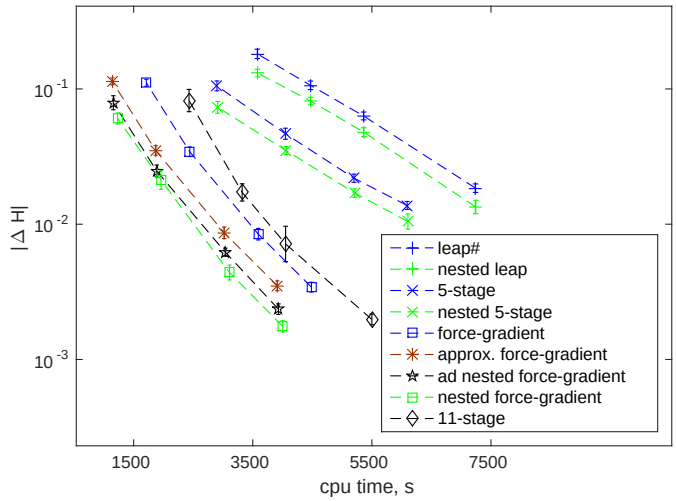

Figure 2: Computational costs for different methods

Figure 2 presents the CPU time, required for the proposed integrators (2.4)–(2.11), versus the achieved accuracy. We can observe that the nested force-gradient method (2.10) and adapted nested force- gradient method (2.11) show much better results in terms of a computational efficiency than the integrators (2.9) and (2.5); and even compared to the 11 stage scheme (2.6). Here we can see that the modification of (2.5) proposed in [17] also performs better than its original version. It shows almost similar computational costs as nested versions of the force-gradient approach (2.10) -(2.11), since it has the same number of D^{-1} (see Table 1). But it is less efficient because the proposed nested approach is more precise.

Integrator:	step size h	M	D^{-1} per step	D^{-1} per trajectory
5 stage method	0.0294	-	6	420
nested 5 stage method	0.0286	700	6	408
5 stage force-gradient	0.0550	-	10	370
approx. force-gradient [17]	0.0540	-	8	290
nested force-gradient	0.0560	450	8	285
adapted nested force-gradient	0.0560	450	8	285
11 stage method	0.0625	-	12	384

Table 1: Step-sizes and number of inversions of D per step and per trajectory for acceptance rate of 90%

Table 1 shows the number of inversions of the Dirac operator D, which is needed to reach 90% acceptance rate of the HMC. Since D^{-1} is the most computationally demanding part it is important to see how many of these inversions are required per each trajectory. From Table 1 it easy to see that the adapted nested force-gradient method (2.11) and nested force-gradient method (2.10) need the least number of D^{-1} per trajectory to reach the chosen acceptance rate $\approx$90%.

We can also claim that methods (2.10) and (2.11) have a potential to perform even better with respect to the computational effort in the case of lattice QCD problems, since the impact of the fermion action (3.3) and the computational time to obtain the inversion of the Dirac operator D is much more significant.

5 Conclusions and outlook

We presented the nested force-gradient approach (2.10) and its adapted version (2.11) applied to a model problem in quantum field theory, the two-dimensional Schwinger model. The derivation of the force-gradient terms was given and the Schwinger model was introduced. Nested force-gradient schemes seem to be an optimal choice with relatively high convergence order and low computational effort. Also it would be possible to improve the algorithm (2.11) by measuring the Poisson brackets of the shadow Hamiltonian of the proposed integrator and then tuning the set of optimal parameters, e. g. micro and macro step sizes.

In future work we will apply this approach to the HMC algorithm for numerical integration in Lattice QCD. Here we expect the adapted nested-force gradient scheme to outperform the original one, if we further partition the action into more than two parts, by using techniques to factorize the fermion determinant: less force-gradient information is needed for the most expensive action, and only leap-frog steps are needed for the high frequency parts of the action.

Acknowledgments

This work is part of project B5 within the SFB/Transregio 55 *Hadronenphysik mit Gitter-QCD* funded by DFG (Deutsche Forschungsgemeinschaft).

References

[1] A. Bazavov et al., Chiral transition and $U(1)_A$ symmetry restoration from lattice QCD using domain wall fermions, Phys. Rev. D 86 (201), 094503.
[2] E. Borici, C. Joó, A. Frommer, Numerical methods in QCD, Springer, Berlin, 2002.
[3] M.A. Clark, B. Joó, A.D. Kennedy, P.J. Silva, Better HMC integrators for dynamical simulations, PoS 323(2010).
[4] N. Christian, K. Jansen, K. Nagai, B. Pollakowski, Scaling test of fermion actions in the Schwinger model, Nuclear Physics B 739 (2006), pp. 60–84.
[5] S. Duane, A.D. Kennedy, B.J. Pendleton, D. Roweth, Hybrid Monte Carlo, Phys. Lett. B195 (1987), pp. 216–222.
[6] E. Hairer, C. Lubich, G. Wanner, Geometric Numerical Integration: Structure-Preserving Algorithms for Ordinary Differential Equations, Springer, Berlin, 2002.
[7] A.D. Kennedy, M.A. Clark, Speeding up HMC with better integrators, PoS 038(2007).
[8] A. D. Kennedy, M. A. Clark, P. J. Silva, Force Gradient Integrators, PoS 021(2009).
[9] A.D. Kennedy, P.J. Silva, M.A. Clark, Shadow Hamiltonians, Poisson Brackets and Gauge Theories, Phys. Rev. D 87 (2013), 034511.
[10] M. Lüscher, S. Schäfer, Lattice QCD with open boundary conditions and twisted-mass reweighting, Comput. Phys. Commun. 184(2013), pp 519–528.
[11] I.P. Omelyan, I.M. Mryglod, R. Folk, Symplectic analytically integrable decomposition algorithms: classification, derivation, and application to molecular dynamics, quantum and celestial mechanics, Comput. Phys. Commun. 151 (2003), pp. 272–314.
[12] J.S. Schwinger, Gauge Invariance and Mass. 2, Phys. Rev. 128 (1962), pp. 2425–2429.
[13] J.C. Sexton, D.H. Weingarten, Hamiltonian evolution for the hybrid Monte Carlo algorithm, Nucl. Phys. B380 (1992), pp. 665–678.
[14] D. Shcherbakov, M. Ehrhardt, Multistep Methods for Lattice QCD Simulations, PoS (Lattice 2011), pp. 327–333.
[15] D. Shcherbakov, M. Ehrhardt, M. Günther, M. Peardon, Force-gradient nested multirate methods for Hamiltonian systems, Comput. Phys. Commun. 187(2015), pp 91–97.
[16] P.J. Silva, A.D. Kennedy, M.A. Clark, Tuning HMC using Poisson brackets, PoS 041(2008).
[17] H. Yin, R. D. Mawhinney, Improving DWF Simulations: the Force Gradient Integrator and the Möbius Accelerated DWF Solver, PoS (Lattice 2011) 051.